SLAC-PUB-9993
June 2003

Controlled Synthesis and Assembly of FePt Nanoparticles

Shouheng Sun *et al.*

Submitted to Journal of Applied Physics

Stanford Linear Accelerator Center, Stanford University, Stanford, CA 94309

Work supported by Department of Energy contract DE–AC03–76SF00515.

Controlled Synthesis and Assembly of FePt Nanoparticles

Shouheng Sun,[*†] *Simone Anders,*[‡] *Thomas Thomson,*[‡] *J. E. E. Baglin,* [‡] *Mike F. Toney,* [‡] *Hendrik F. Hamann,*[†] *C. B. Murray,*[†] *Bruce D. Terris* [‡]

IBM T. J. Watson Research Center, Yorktown Heights, New York 10598 and IBM Almaden Research Center, 650 Harry Road, San Jose, California 95120.

Abstract: Monodisperse 4 nm FePt magnetic nanoparticles were synthesized by superhydride reduction of $FeCl_2$ and $Pt(acac)_2$ at high temperature, and thin assemblies of FePt nanoparticles with controlled thickness were formed through polymer mediated self-assembly. Adding superhydride ($LiBEt_3H$) to the organic solution of $FeCl_2$ and $Pt(acac)_2$ in the presence of oleic acid, oleylamine and 1,2-hexadecanediol at 200°C, followed by refluxing at 263°C, led to monodisperse 4 nm FePt nanoparticles. The initial molar ratio of the metal precursors was retained during the synthesis; and the final FePt composition of the particles was readily tuned. Alternatively absorbing a layer of polyethylenimine (PEI) and the FePt nanoparticles onto a solid substrate resulted in nanoparticle assemblies with tunable thickness. Chemical analysis of the assemblies revealed that more iron oxide was present in the thinner assemblies annealed at lower temperature or for shorter time. Thermal annealing induced the internal particle structure change from chemically disordered fcc to chemically ordered fct and transformed the thin assembly

---

* To whom correspondence should be addressed. E-mail: ssun@us.ibm.com.

† IBM T. J. Watson Research Center.

‡ IBM Almaden Research Center.

from superparamagnetic to ferromagnetic. This controlled synthesis and assembly can be used to fabricate FePt nanoparticle-based functional devices for future nanomagnetic applications.

Introduction

Controlled synthesis and assembly of small hard magnetic particles has attracted great interest due to their potential applications in ultrahigh density magnetic recording,[1,2] highly sensitive magnetic sensors[3,4] and advanced nanocomposite permanent magnets.[5] The hard magnetic FePt materials are excellent candidates for these particle-based applications. They are more chemically stable than other well-known hard magnetic materials such as CoSm, NdFeB, and have very high magnetocrystalline anisotropy, K_u. In an ordered intermetallic phase, their K_u can reach values as high as 10^8 erg/cm^3,[6] indicating that the magnetic anisotropy energy K_uV of a single magnetic grain (V is the magnetic grain volume) is much larger than the thermal fluctuation energy k_BT (k_B is the Boltzman's constant, and T is the temperature) at ambient condition, and an FePt particle with a diameter as small as 3 nm is still thermally stable and ferromagnetic. Recent advance in magnetic recording technology has indicated that if self-assembled in a tightly packed, exchange-decoupled array with control of magnetic easy axis direction, these FePt nanoparticles could support high-density magnetization reversal transitions and would be ideal candidate for future ultra-high density data storage media, with potentially one bit per particle.[2,7]

To use self-organized FePt nanoparticles for magnetic recording applications, a practical route to monodisperse ferromagnetic FePt nanoparticles and nanoparticle assemblies with controlled assembly thickness and surface roughness is needed. Solution phase-based high temperature decomposition of $Fe(CO)_5$, and reduction of platinum acetylacetonate, $Pt(acac)_2$, was recently developed to make monodisperse FePt nanoparticles,[8-11] and has been demonstrated to be a general approach to other multi-component nanoparticles, including binary FeMo,[12] and tertiary CoFePt[13] and AgFePt[14] nanoparticles. However, for future practical applications, several issues regarding this decomposition/reduction process

need to be addressed. The $Fe(CO)_5$ is volatile, and is thermally unstable, gradually releasing CO and Fe at ambient temperature, rendering $Fe(CO)_5$ a well-known toxic chemical. The high temperature nature of the synthesis needs excess of $Fe(CO)_5$ in the synthesis. A correlation between the molar ratio of $Fe(CO)_5/Pt(acac)_2$ and FePt composition always needs to be established in order to determine the final composition of the particles.[9] Furthermore, for nanoparticles to store magnetic information, they have to be arranged in a smooth thin assembly with a thickness of ~10 nm for over 100 Gbit/in^2 recording.[15] It is therefore desired that the synthesis use a less toxic metal precursors; the initial molar ratio of metal precursors be carried over to the final product; and the nanoparticles be assembled with control on assembly thickness.

We report a simple chemical process of synthesizing FePt nanoparticles by reduction of $FeCl_2$ and $Pt(acac)_2$ at 200°C, followed by refluxing at 263°C. The particle growth is self-limited and 4 nm FePt nanoparticles are readily separated. The initial molar ratio of the metal precursors is carried over to the final product, and the FePt composition is easily tuned. We further demonstrate that alternate adsorption of polyethylenimine (PEI) and FePt nanoparticles on a HO-terminated surface via surface ligand exchange leads to 4 nm FePt nanoparticle assemblies with controlled thickness. Thermal annealing is applied to control structural and magnetic properties of the assemblies. This controlled synthesis and assembly of FePt nanoparticles offers a convenient route to future fabrication of FePt nanoparticle-based devices.

Experimental Section

The synthesis was carried out using standard airless procedures and commercially available reagents. Absolute ethanol, hexane, and chloroform were used as received. Tetrahydrofuran (THF) solution of superhydride ($LiBEt_3H$) (1M), phenyl ether (99%), 1,2-hexadecanediol (97%), oleic acid (90%), and iron (II) chloride tetrahydrate ($FeCl_2 \cdot 4H_2O$) were purchased from Aldrich Chemical

Company. Oleylamine was from Fluka; and platinum acetylacetonate, $Pt(acac)_2$, was from Strem Chemicals, Inc.

Synthesis of $Fe_{58}Pt_{42}$ nanoparticles. In a flask equipped with N_2 in/outlet, septa rubber, thermal probe were added $Pt(acac)_2$ (197 mg, 0.5 mmol), $FeCl_2 \cdot 4H_2O$ (139mg, 0.70 nmmol), 1,2-hexadecanediol (520 mg, 2 mmol) and phenyl ether (25 mL) under nitrogen atmosphere. The mixture was heated to 100°C for 10 min. Oleic acid (0.16 mL, 0.5 mmol) and oleylamine (0.17 mL, 0.5 mmol) were added; and the mixture was continuously heated to 200°C for 20 minutes. $LiBEt_3H$ (1 M THF solution, 2.5 mL) was slowly dropped into the mixture in a duration of ~2 minutes. The black dispersion was stirred at 200°C for 5 minutes under N_2 to remove low boiling solvent, and under a blanket of N_2 was heated to reflux at 263°C for 20 minutes. The heating source was removed and the black reaction mixture was cooled to room temperature. Ethanol (40 mL) was then added under ambient condition. The black product was precipitated and separated by centrifugation (6000rpm, 10 minutes). The yellow-brown supernatant was discarded and the black product was dispersed in hexane (~20 mL) in the presence of oleic acid (~0.05 mL) and oleylamine (~0.02 mL). Any unsolved precipitation was removed by centrifugation (6000 rpm, 10 minutes). The product was then precipitated out by adding ethanol (~20 mL) and separated with centrifugation (6000rpm, 10 minutes). It was once again dispersed in hexane in the presence of oleic acid and oleylamine, precipitated out by adding ethanol and separated with centrifugation. The product, $Fe_{58}Pt_{42}$ nanoparticles, was re-dispersed in hexane solvent for further use.

Similarly, 0.61 mmol of $FeCl_2$ and 0.5 mmol $Pt(acac)_2$ led to $Fe_{55}Pt_{45}$ nanoparticles; and 0.5 mmol of $FeCl_2$ and 0.5 mmole $Pt(acac)_2$ to $Fe_{50}Pt_{50}$ nanoparticles.

Nanoparticle assembly. A naturally oxidized silicon substrate was cleaned using ethanol and dried under a flow of N_2. The substrate was then immersed into the chloroform solution of PEI (~20 mg/mL) for about 30 seconds, withdrawn from the solution and dipped into ethanol solvent to wash off extra PEI on the substrate surface and dried. The PEI functionalized substrate was immersed into the

hexane dispersion of FePt nanoparticles for 30 seconds, withdrawn from the dispersion, rinsed with fresh hexane and dried. This yielded one layer of PEI/FePt assembly. By repeating the coating of PEI and FePt, the multilayer of 4 nm FePt nanoparticle assembly was easily made.

Thermal annealing of the FePt nanoparticle assemblies. The PEI/FePt assemblies were thermally annealed for further characterization. The annealing transforms the particle structure from the chemically disordered fcc phase to the chemically ordered fct phase, rendering FePt nanoparticles with desirable high magnetocrystalline anisotropy and ferromagnetism at room temperature.[8] Further, the annealing also results in the decomposition of the PEI and oleic acid/oleylamine left around FePt particles into carbonaceous matrix, yielding smooth FePt nanoparticle assemblies. The annealing was performed in an inert atmosphere (N_2 or He), or under Ar + H_2(5%) in a quartz tube at temperatures ranging from 400°C to 800°C and durations between 2 min and 2h.

Nanoparticle characterization. Fe and Pt elemental analyses of the as-synthesized FePt nanoparticle powders were performed on inductively coupled plasma - optic emission spectrometry (ICP-OES) at Galbreith Lab, Tennessee. The particles were precipitated from their hexane dispersion by ethanol, washed with ethanol and dried. Composition and thickness of the FePt nanoparticle assembly were determined by Rutherford backscattering spectrometry (RBS).

Samples for transmission electron microscopy (TEM) analysis were prepared by drying a hexane dispersion of FePt particles on amorphous carbon coated copper grids. Particle size was determined using a Philips CM 12 TEM (120 KV). The thin-layered PEI/FePt assembly was imaged using CM 12 TEM with the assembly on silicon oxide coated copper grids. The layered structure on thermally oxidized silicon (100) substrate was characterized by X-ray reflectivity (XRF) measurements of the films. The measurements were conducted using $CuK_{\alpha 1}$ radiation from an 18 kW X-ray generator, monochromatized with flat Ge(111) crystal. The background (diffuse) scattering was subtracted from the raw data to yield the true specular reflectivity. Digital Nanoscope IIIa in multimedia mode was used for Atomic force microscopy (AFM) analysis of the surface morphology of the layered assembly.

The chemical nature of the films was studied using Near Edge X-ray Absorption Fine Structure (NEXAFS) spectroscopy. The experiments were performed at the Advanced Light Source at beamline 7.3.1.1. that is equipped with a spherical grating monochromator and has an energy resolution of $E/\Delta E=1800$. X-ray diffraction (XRD) measurements were performed in grazing incidence geometry at the National Synchrotron Light Source using beamline X20C. The diffracted beam was analyzed with 1 milliradian Soller slits, which provided a resolution much smaller than any of the diffraction peak widths.

Magnetic studies were carried out using a MPMS2 Quantum Design SQUID magnetometer with fields up to 5 T and temperatures from 5°K to 350°K, and Vibrating sample magnetometer with field up to 9 T at room temperature. Measurements were done on variously layered FePt nanoparticle assemblies on thermally oxidized p-type silicon (100) substrates.

Results and Discussion

Synthetic issues. As illustrated in Figure 1, the reduction of $FeCl_2$ and $Pt(acac)_2$ mixture by superhydride in the presence of oleic acid, oleylamine and 1,2-hexadecanediol at 200°C, followed by refluxing at 263°C, led to monodisperse 4 nm FePt nanoparticles. Although the reduction was usually performed at 200°C, experimental results show that superhydride could be added at any temperature in the range between 200°C and 263°C. Adding the reducing agent at lower temperature (<200°C) did not yield high quality FePt nanoparticle materials.

Two metal precursors, $FeCl_2$ and $Pt(acac)_2$, were specifically chosen for this reduction process as they formed clear phenyl ether solution when mixed. Presumably, the mixing of $FeCl_2$ and $Pt(acac)_2$ resulted in an $FeCl_2$-$Pt(acac)_2$ intermediate that facilitated the formation of FePt nanoparticles under the current reaction condition. Other combination of Fe salt, such as $FeCl_3$, $Fe(acac)_3$, and Pt salt, such as $PtCl_2$, K_2PtCl_4, did not yield good quality FePt nanoparticles. The $FeCl_2$ used in the reaction can be in either anhydrous state or hydrated state. If $FeCl_2{\cdot}4H_2O$ was used, the mixture was usually stirred at

200°C under nitrogen for about 20 minutes before reducing agent, superhydride, was added to the mixture.

Several different reducing agents have been tested for the reduction process. Metal naphthalides are very powerful reducing agents but are also difficult to store due to their extremely air- and moisture-sensitive nature. Polyalcohol, such as ethylene glycol and 1,2-hexanedecanediol, or the other long chain alkyl alcohols, are not a strong reducing agent for the $FeCl_2$-$Pt(acac)_2$ reduction. But the alkyl alcohol can act like a co-surfactant, and help to generate FePt nanoparticles with better quality. Metal borohydrides are a class of well-known reducing agents for the reduction of various metal salts to metal nanoparticles.[16-19] Specifically, derivative borohydride, such as superhydride, $LiBEt_3H$, is easily dissolved in organic ether solvent, facilitating homogenous reduction of metal salt and formation of metal nanoparticles.[20-23] The advantage of choosing $LiBEt_3H$ over other metal borohydrides is as follows: (i) Li^+ cation from the superhydride can combine with Cl^- or $acac^-$ from $FeCl_2$ and $Pt(acac)_2$ to form Li salt that is easily washed off from the product with alcohol; (ii) after reduction, BEt_3 is released as a whole molecule: it may be removed from the system under nitrogen, or it can combine with other organic ether/amine/alcohol species in the mixture, to form organic adducts, leading to pure FePt nanoparticles.

The binary FePt nanoparticles are stabilized by oleic acid and oleylamine as in the previous decomposition/reduction process. If the final product is Fe-rich, then a combination of oleic acid/oleylamine with the ratio of > 1 is needed for particle stabilization during the purification process. If the final product is Pt-rich, then a combination of oleic acid/oleylamine with the ratio of < 1 is required for the stabilization. This indicates that the excess fraction of Fe or Pt atoms is located at surface positions of the FePt particles.

Under the current reaction condition, the particle growth is self-limited. The size of the particles is independent of the amount of stabilizers present, the addition rate of reducing agent, reduction temperature (from 200°C to 263°C), and refluxing time (from 30 minutes to 2h). 4 nm FePt particles

were always separated. Refluxing may not be necessary, but it did help to yield FePt nanoparticles with better shape. Figure 2 is the TEM image of 4 nm FePt nanoparticles deposited on an amorphous carbon copper grid from their hexane dispersion. It can be seen that FePt nanoparticles are uniform with narrow size distribution.

Elemental analysis. Fe, Pt elemental analysis of the FePt powder sample show that the mixture of 0.75 mmol of $FeCl_2$ and 0.5 mmol $Pt(acac)_2$ yielded $Fe_{60}Pt_{40}$. Similarly, 0.70 mmol of $FeCl_2$ and 0.5 mmol $Pt(acac)_2$ led to $Fe_{58}Pt_{42}$, and 0.5 mmol of $FeCl_2$ and 0.5 mmole $Pt(acac)_2$ to $Fe_{50}Pt_{50}$. Within ICP detection limit, these FePt composition data match exactly with those from the calculated ones according to the molar ratio of two metal precursors. RBS on self-assembled FePt thin films also confirmed that each kind of FePt nanoparticles has the composition close to the calculated one. For example, RBS analyses on different assemblies of $Fe_{60}Pt_{40}$ nanoparticles would usually result in ratios of $Fe_{(59-61)}Pt_{(41-39)}$. These compositional analyses on FePt nanoparticles indicate that in this reduction method, the initial metal molar ratio is carried over to the final product, and the FePt composition is easily controlled.

Polymer mediated FePt nanoparticle assembly. The oleic acid/oleylamine coated FePt nanoparticles can be readily dispersed into hexane or chloroform solvent, facilitating surface ligand exchange and controlled nanoparticle assembly. The ligand exchange experiments show that various functional polymers can replace oleic acid/oleylamine around these nanoparticles to give polymer nanoparticle composites. For example, mixing chloroform solution of polyethylenimine (PEI) with hexane dispersion of FePt led to PEI-FePt nanocomposite that is not soluble in hexane. By exchanging the stabilizers bound to the particles with multifunctional polymers that attach to a substrate, the polymer and FePt nanoparticles can be alternatively adsorbed onto substrate, and an FePt assembly with controlled thickness can be made. This polymeric molecule-assisted nanoparticle assembly is a well-known technique to polymer nanoparticle nanocomposites.[24-31] Densely packed self-assembled polymeric monolayer is usually obtained by spontaneous adsorption of surfactant molecules from

organic solution onto a solid substrate via hydrogen bonding, ionic bonding or covalent bonding. PEI has been found to be adsorbed on HO-terminated substrate, and used for gold nanoparticle assembly on mica, silicone oxide and glass surface.[32] The assembly of FePt nanoparticles into a macroscopic two-dimensional array on a PEI-functionalized substrate is depicted in Figure 3A.[33] The assembly process includes: (1) surface functionalization with a layer of PEI coating; and (2) replacement of the particle stabilizers with a pedant functional –NH- group of the PEI. The pendant functional group –NH- extends out in the solution. By dipping the PEI-derivative substrate into the particle dispersion, ligand exchange at the PEI surface occurs and a monolayer FePt particle assembly is formed. Figure 3B shows a TEM image of one layer of 4 nm $Fe_{58}Pt_{42}$. By repeating this simple two-step process in a cyclic fashion, a PEI/FePt multilayer assembly can be obtained. Figure 3C shows a TEM image of 3 layers of 4 nm $Fe_{58}Pt_{42}$ nanoparticles self-assembled on a PEI-modified silicon oxide surface. Further experiments show this PEI-mediated assembly can be made on virtually any size and shaped HO-terminated substrates.

General analysis of the assemblies. For a series of 2-, 3-, 5-layered FePt nanoparticle assemblies, the depth profiling of both Fe and Pt obtained from RBS measurements is consistent with that predicted from the actual number of layers of FePt nanoparticles. The sample contains Fe, Pt and other C, O, N components. The overall coating thickness for a 3-layer 4 nm FePt assembly is estimated to be in the region of 10 – 15 nm, depending on the density and H content (not determined). The layered structure is further analyzed by X-ray reflectivity analysis of nanoparticle assemblies. In X-ray reflectivity the reflected X-ray intensity is measured as a function of incidence angle and the data are analyzed using a multilayer model that incorporates several parameters which are varied to produce the best fit to the data.[34] X-ray reflectivity measures the electron density of the nanoparticle assembly, which can be converted into mass density. The result of this analysis for a 3-layer assembly is shown in Figure 4, which plots mass density as a function of position from the silicon substrate surface. The three layers are readily evident as regions of larger mass density than the PEI between the nanoparticle layers. The spacings between the first-second and second-third layers are both 6.5 nm. These data demonstrate the

layering associated with the nanoparticle assembly. Atomic force microscopy (AFM) analyses of various 3-layer thin assemblies indicate smooth assembly surface. Figure 5 is the AFM image of a 3-layer $Fe_{58}Pt_{42}$ assembly annealed at 550°C for 30 min on a microslide substrate. The root mean square (RMS) variation in height over areas of 9.4 x 9.4 μm is at 3.1 nm.

Chemical analysis of the assemblies. The chemical nature of the annealed films was studied using near edge X-ray absorption fine structure (NEXAFS) spectroscopy.[35] Tunable photons from a synchrotron radiation beamline can be used to study the X-ray absorption of a material as a function of photon energy. The X-ray absorption spectrum is element specific and fine structure of the absorption edges reflects the bonding environment of the element in the compound.[35] NEXAFS data of Fe absorption on the annealed thin FePt nanoparticle assemblies indicate that all assemblies contain both metallic iron and iron oxide.[36] The iron/iron oxide fraction varies for different assemblies and depends on the FePt particle assembly thickness and annealing history of the assembly. More metallic Fe exists in a thicker assembly. For the assemblies with the same thickness, more metallic Fe is found in the assembly annealed at higher temperature or for longer time. Figure 6 shows NEXAFS spectra of the Fe L_3 and L_2 absorption edges of the 3-layers assemblies annealed at 725°C in He atmosphere for various durations together with reference spectra of metallic Fe and Fe_3O_4. It shows that with increasing annealing duration (Fig. 6A-C), the peaks corresponding to metallic Fe are increased while those to iron oxide are decreased, indicating more metallic iron is present in the assembly. Simulation based on the superposition of Fe and Fe_3O_4 (Fig. 6D,E) can fit well to the observed spectra. For example, the observed spectrum for the 120 min annealed assembly (Fig. 6C) corresponds to a superposition of 75%Fe/25%Fe_3O_4.[37] Assuming the particle consists of a FePt core and an oxide shell and using typical literature values for the electron escape depth for carbon (10 nm), metal (1.5 nm), and metal oxides (5 nm),[35,38] we can estimate that the relative 75%Fe/25%Fe_3O_4 contribution to the spectrum comes from a particle with and average 0.1 nm thick oxide shell and a 3.8 nm metallic particle core. Although the accurate electron escape depths in our sample is not available, preventing us from getting the exact

number of iron/iron oxide fraction, the estimate shows that a very thin oxide shell is indeed present in the assemblies. The chemical origin of the iron oxide is easily understood considering the fact that both the decomposition of the iron oleate on a FePt particle surface during the annealing and air oxidation of the surface iron atom of an annealed FePt particle will all lead to iron oxide.

Structural analysis of the assemblies. The crystal structure of the FePt nanoparticles in a thin assembly was determined by the X-ray diffraction (XRD). The XRD of the as-synthesized FePt particles reveals a typical chemically disordered fcc structure,[8] in which Fe atoms are substituted into Pt positions and vice versa. Annealing induces the Fe and Pt atoms to rearrange into the long range chemically ordered fct structure, which can be viewed as a natural superlattice of alternating Fe and Pt atomic planes. The change of the internal particle structure upon annealing depends on annealing temperature and duration, as well as the Fe/Pt ratio. The onset of this phase change occurs at about 500°C, which is consistent with previous observation on FePt nanoparticles prepared from the decomposition/reduction process.[8,39,40] Figure 7 shows in-plane X-ray diffraction scans for the as-synthesized 3-layer $Fe_{58}Pt_{42}$ assembly (Fig. 7A) and for the one annealed for 2 minutes in He atmosphere at 725°C in He atmosphere (Fig. 7B). Figure 7B shows the typical superlattice peaks of (001) and (110) that are characteristic of the ordered FePt ($L1_0$) compound phase.[6] The one-dimensional chemical ordering parameters S can be obtained from the ratio of the peak intensity of the superlattice peaks to the fundamental peaks.[41] S is unity for perfectly ordered films, and is zero for a chemically disordered film. This order parameter depends on the annealing history of the sample. Figure 8A illustrates the increase of the S with annealing time at 725°C. It shows that for the as synthesized assembly the order parameter is zero and is increased up to almost 1 for the sample annealed for 2 h duration. The order parameter also varies with annealing temperature at the same annealing time. It increases with temperature from 0.6 at 500°C for 5 min to 0.8 at 800°C for 5 min.

Annealing induced particle aggregation. High temperature annealing also leads to particle aggregation. Previous in-situ TEM experiments have shown clear coalescence of FePt particles annealed

at 600°C under high vacuum for 1 h.[40] From the line width of the (111) peak it is also possible to estimate the (111) coherence length that is related to the particle diameter.[42] Figure 8B shows the (111) coherence length *vs.* annealing time at annealing temperature 725°C. For the 2 min annealed assembly the coherence length has increased from 2.8 nm for the as synthesized assembly to 8 nm, and it increases further with annealing duration. The average particle size increases also with annealing temperature. The particle size estimated from XRD line width for 3 layer assemblies annealed at 580°C for 30 min is 5 nm but rises to 17 nm for a 800°C/5 min. annealed sample. To prevent agglomeration of the FePt nanoparticles, ion beam irradiation of the as-synthesized FePt nanoparticle assemblies, followed by thermally annealing, was applied to treat the thin assembly. Preliminary experiments showed that this treatment improved particles' ability against aggregation during annealing process.

Magnetic properties of the assemblies. Along with the structural change, the magnetic properties of the assemblies can be easily tuned. The as-synthesized FePt nanoparticles have chemically disordered fcc structure, and the related thin assemblies are superparamagnetic at room temperature with $H_c = 0$. The thermal annealing transforms the chemically disordered fcc structure to the chemically ordered fct structure, rendering ferromagnetic thing FePt nanoparticle assemblies. The coercivity of the annealed thin films increases with annealing time and temperature, and a minimum annealing temperature of about 500°C under an inert atmosphere is required to form ferromagnetic thin films. This corresponds to the structure transformation from fcc to fct phase at this temperature. On the other hand, the coercivity of the annealed thin films is also dependent on assembly thickness. The thinnest layers that showed coercivity of ~ 300 Oe were 2 layer films for the 4 nm $Fe_{58}Pt_{42}$ particles. This is likely due to the iron/iron oxide ratio variation with the assembly thickness, as observed using NEXAFS. Figure 9 shows the room temperature hysteresis loops of three different 3-layer 4 nm $Fe_{58}Pt_{42}$ nanoparticle assemblies, with Fig. 9A being from as-synthesized assembly and Fig. 8B,C being from the annealed assemblies in He at 725°C for 2 min and 20 min respectively. For 2 min annealed sample, its coercivity is 2000 Oe and remanent magnetization M_r close to 0.5 M_s, where M_s is the saturation magnetization,

while for 20 min annealed sample, its H_c reaches 7000 Oe and M_r/M_s is clearly larger than 0.5, indicating particle aggregation and strong exchange-coupling among the neighboring particles.[43] This is consistent with the high temperature particle aggregation indicated by (111) coherence length increase measured by XRD.

The magnetic properties of the thin FePt nanoparticle assemblies can be further improved by annealing the assembly under Ar + 5%H_2 as the reducing atmosphere can reduce iron oxide layer present around FePt nanoparticles. Magnetic measurements show that a 3-layer $Fe_{58}Pt_{42}$ assembly annealed at 450°C is ferromagnetic with coercivity reaching 800 Oe. Further experiments on this reductive annealing and its application in fabricating thin FePt assemblies with large H_c are underway.

Conclusions

We have reported that superhydride reduction of $FeCl_2$ and $Pt(acac)_2$ in the presence of oleic acid, oleylamine and 1,2-hexadecanediol can be used to make 4 nm FePt nanoparticles. The initial molar ratio of two metal precursors is carried over to the final product, and the composition of final FePt is easily tuned. Alternatively absorbing a layer of polyethylenimine and the FePt nanoparticles onto a solid substrate results in FePt nanoparticle assemblies with tunable thickness. Thermal annealing induces the internal particle structure from chemically disordered fcc to chemically ordered fct and transforms the thin assembly from superparamagnetic to ferromagnetic. The reported synthesis of FePt nanoparticle with controlled size and composition, and PEI-mediated self-assembly of FePt nanoparticles with tunable thickness offers a convenient process of fabricating FePt nanoparticle based functional devices for various magnetic applications.

Acknowledgement. We thank A. J. Kellock for RBS measurements.

References

(1) Weller, D.; Moser, A. *IEEE Trans. Magn.* **1999**, *35*, 4423.

(2) Weller, D.; et al *IEEE Trans. Magn.* **2000**, *36*, 10.

(3) Liu, S. H. *IEEE Trans. Mag.* **1999**, *35*, 3989.

(4) Sqalli, Q.; Brenal, M. P.; Hoffmann, P.; Marquis-Weible, F. *Appl. Phys. Lett.* **2000**, *76*, 2134.

(5) Kneller, E. F.; Hawig, R. *IEEE Trans. Magn.* **1991**, *27*, 3588.

(6) Farrow, R. F. C.; et al *J. Appl. Phys.* **1996**, *79*, 5967.

(7) Moser, A.; et al *J. Phys. D: Appl. Phys.* **2002**, *35*, R157.

(8) Sun, S.; Murray, C. B.; Weller, D.; Folks, L.; Moser, A. *Science* **2000**, *287*, 1989.

(9) Sun, S.; Fullerton, E. E.; Weller, D.; Murray, C. B. *IEEE Trans. Magn.* **2001**, *37*, 1239.

(10) Harrell, J. W.; Wang, S.; Nikles, D. E.; Chen, M. *Appl. Phys. Lett.* **2001**, *79*, 4393.

(10) Stahl, B.; et al. *Adv. Mater.* **2002**, *14*, 24.

(12) Li, Y.; Liu, J.; Wang, Y.; Wang, Z. L. *Chem. Mater.* **2001**, *13*, 1008.

(13) Chen, M.; Nikles, D. E. *Nanolett.* **2002**, *2*, 211.

(14) Kang, S.; Harrell, J. W.; Nikles, D. E. *Nanolett.*, **2002**, in press.

(15) Wood, R. *IEEE Trans. Magn.* **2000**, *36*, 36.

(16) Schlesinger, H. I.; et al *J. Am. Chem. Soc.***1953**, *84*, 1493.

(17) Yiping, L.; Hadjipanayis, G. C.; Sorensen, C. M.; Klabunde, K. J. *J. Magn Mag Mater.* **1989**, *79*, 321.

(18) Glavee, G. N.; Klabunde, K. J.; Sorensen, C. M.; Hadjipanayis, G. C. *Langmuir* **1994**, *10*, 4726.

(19) Sun, Y.-P.; Rollins, H. W.; Guduru, R. *Chem. Mater.* **1999**, *11*, 7.

(20) Bonnemann, H.; Brijoux, W.; Joussen, T. *Angew. Chem. Int. Ed. Engl.* **1990**, *29*, 273.

(21) Bonnemann, H.; Brinkmann, R.; Koppler, R.; Neiteler, P.; Richter, J. *Adv. Mater.***1992**, *4*, 804.

(22) Sun, S.; Murray, C. B. *J. Appl. Phys.* **1999**, *85*, 4325.

(23) Sun, S.; Murray, C. B.; Doyle, H. *Mat. Res. Soc. Symp. Proc.* **1999**, *577*, 385.

(24) Fendler, J. H. *Chem. Mater.* **1996**, *8*, 1616.

(25) Liu, Y.; Wang, A.; Claus, R. *J. Phys. Chem. B* **1997**, *101*, 1385.

(26) Cassagneau, T.; Mallouk, T. E.; Fendler, J. H. *J. Am. Chem. Soc.* **1998**, *120*, 7848.

(27) Aliev, F. G. et al. *Adv. Mater.* **1999**, *11*, 1006

(28) Rogach, A. L.; Koktysh, D. S.; Harrison, M.; Kotov, N. A. *Chem. Mater.* **2000**, *12*,1526.

(29) Halaoui, L. I. *Langmuir* **2001**, *17*, 7130.

(30) Kotov, N. A. *MRS Bulletin* **2001**, 992.

(31) Hicks, J. F.; Seok-Shon, Y.; Murray, R. W. *Langmuir* **2002**, *18*, 2288.

(32) Schmitt, J.; Mächtle, P.; Eck, D.; Möhwald, H.; Helm, C. A. *Langmuir* **1999**, *15*, 3256.

(33) Sun, S.; et al. *J. Am. Chem. Soc.* **2002**, *124*, 2884.

(34) Holy, V.; Pietsch, U.; Baumbach, T. in *High-Resolution X-ray Scattering from Thin Films and Multilayers*, Springer-Verlag, Berlin, 1998.

(35) Stöhr, J. *NEXAFS Spectroscopy*, Springer, Berlin 1992.

(36) Anders, S.; et al. *Microelectronic Engineering* **2002**, *61/62*, 569.

(37) Other forms of iron oxide, such as Fe_2O_3, may also exist in the assembly. Due to the surface sensitivity of NEXAFS and the similarity of iron oxide spectra, exact nature of iron oxide in the assembly is difficult to determine.

(38) Regan, T. J.; et al. *Phys. Rev. B* **2001**, *64*, 214422.

(39) Weller, D.; Sun, S.; Murray, C. B.; Folks, L.; Moser, M. *IEEE Trans. Magn.* **2001**, *37*, 2185.

(40) Dai, Z. R.; Sun, S.; Wang, Z. L. *Nanolett.* **2001**, *1*, 443.

(41) Cebollada, A.; Farrow, R. F. C.; Toney, M. F. in *Magnetic Nanostructures*, Ed. H. S. Nalva, American Scientific Publishers, **2002**, pp93.

(42) Klug, H. P.; Alexander, L. E. *X-Ray diffraction Procedures for Polycrystalline and Amorphous Materials*, John Wiley & Sons: New York, **1962**, pp491-538.

(43) Zeng, H.; Sun, S.; Vedantam, T. S.; Liu, J. P.; Dai, Z. R.; Wang, Z. L. *Appl. Phys. Lett.* **2002**, *80*, 2583.

Figure Captions

Figure 1 Schematic illustration of FePt nanoparticle synthesis by superhydride reduction of $FeCl_2$ and $Pt(acac)_2$ in the presence of oleic acid, oleylamine and 1,2-hexadecanediol.

Figure 2 Bright field TEM image of a 2-D array of 4 nm FePt nanoparticles. The assembly was obtained with depositing FePt hexane dispersion on an amorphous carbon coated copper grid and evaporating hexane at room temperature.

Figure 3 (A) Schematic illustration of polymer-mediated self-assembly of FePt nanoparticles by alternatively absorbing a layer of polymer (PEI) and a layer of nanoparticles on a solid surface; and TEM images of PEI-mediated assembly of 4 nm $Fe_{58}Pt_{42}$ nanoparticles on silicon oxide coated copper grids: (B) one layer assembly and (C) three layer assembly.

Figure 4 Mass density of a 3-layer FePt assembly, deduced from the XRF measurement, as a function of position from the silicon substrate (z). The silicon surface is arbitrarily defined as z=0.

Figure 5 AFM image (9.4 x 9.4 μm^2) of a 3-layer 4 nm $Fe_{58}Pt_{42}$ nanoparticle assembly annealed at 530°C under Ar + H_2 (5%) for 30 minutes.

Figure 6 NEXAFS spectra of the Fe L_3 and L_2 absorption edges of 3-layer $Fe_{58}Pt_{42}$ assemblies annealed in He for various durations: (A) 2 min., (B) 20 min, and (C) 120 min, and of the reference thin films of (D) Fe_3O_4 and (E) metallic Fe.

Figure 7 XRD scans of 3-layer $Fe_{58}Pt_{42}$ assemblies. (A) As-synthesized 3-layer assembly; and (B) 3-layer assembly annealed at 725°C for 2 min in He atmosphere, in which the diffraction peaks are indexed following the fct structure.

Figure 8 (A) Fe, Pt order parameter, S and (B) (111) coherence length of the FePt particles as a function of annealing duration. The data were extracted from the XRD scans of the 3-layer $Fe_{58}Pt_{42}$ nanoparticle assemblies annealed in He at 725°C.

Figure 9 In-plane hysteresis loops of 3-layer $Fe_{58}Pt_{42}$ nanoparticle assemblies measured by VSM at room temperature: (A) as-synthesized, and annealed for (B) 2 min and (C) 20 min in He at 725°C.

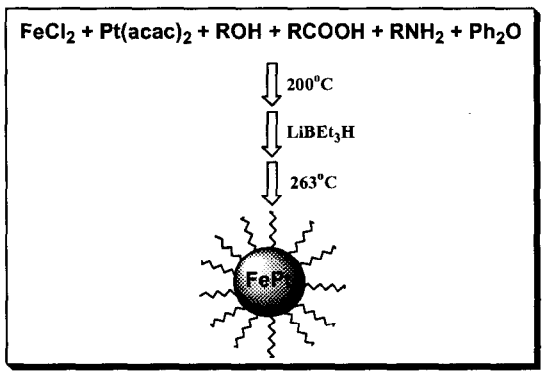

Sun et al, Figure 1

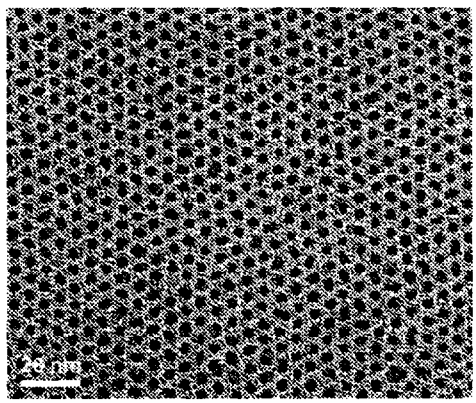

Sun et al, Figure 2

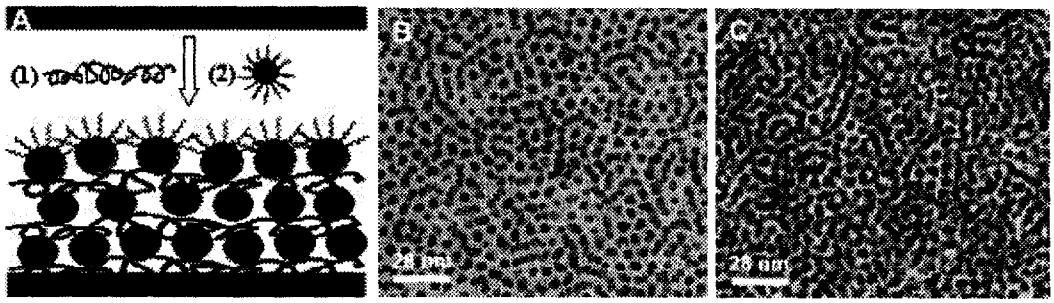

Sun et al, Figure 3

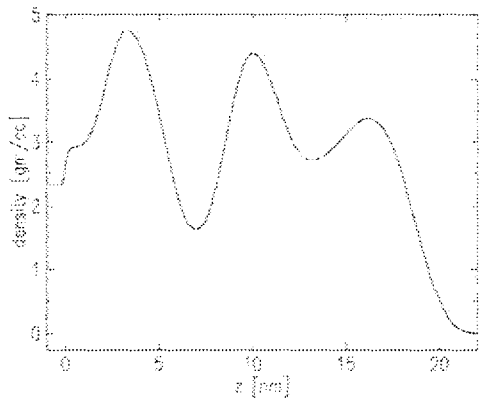

Sun et al, Figure 4

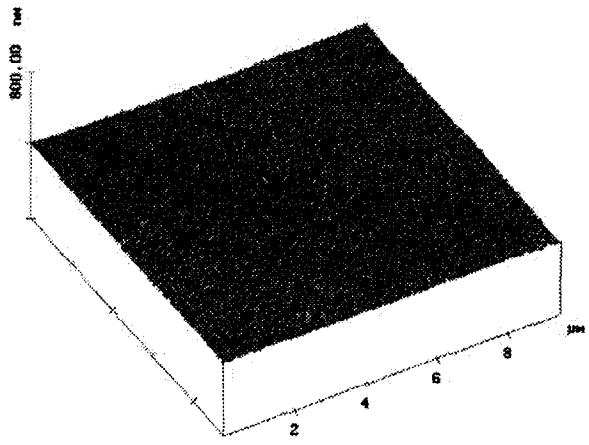

Sun et al, Figure 5

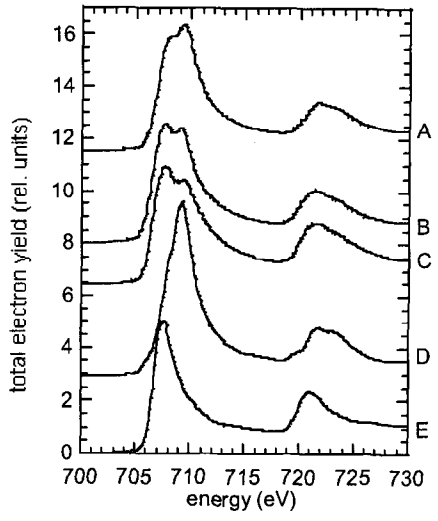

Sun et al, Figure 6

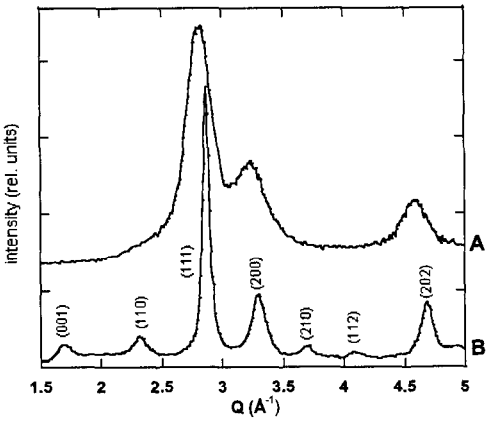

Sun et al, Figure 7

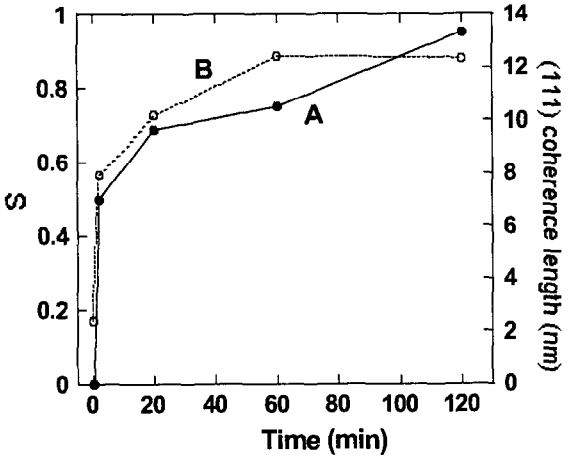

Sun et al, Figure 8

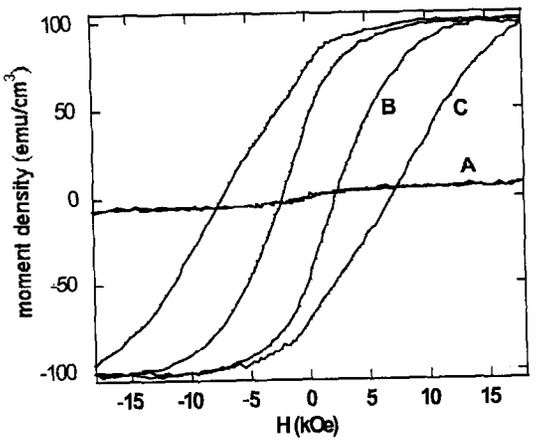

Sun et al, Figure 9